



Enhanced magnetism of perovskite oxides, $\text{Sr}(\text{Sn},\text{Fe})\text{O}_{3-\delta}$, by substitution of nonmagnetic Ca and Ti ions

Kiyoshi Nomura¹ · Shigeyo Suzuki¹ ·
Tomoya Mizunuma¹ · Yuya Koike¹ ·
Atsushi Okazawa²

© Springer International Publishing AG 2017

Abstract Magnetic properties of perovskite oxides, $\text{SrSn}_{1-x}\text{Fe}_x\text{O}_{3-\delta}$ ($x \leq 0.15$), substituted with nonmagnetic Ca and Ti ions were studied. XRD patterns showed the orthorhombic structure (close to tetragonal) of $(\text{Sr}_{1-y}\text{Ca}_y)(\text{Sn}_{1-x}\text{Fe}_x)\text{O}_{3-\delta}$ and $\text{Sr}(\text{Sn}_{1-x-y}\text{Fe}_x\text{Ti}_y)\text{O}_{3-\delta}$. The cell volumes decreased with the increase of Ca and Ti doping rates. Although Ti-substituted $\text{Sr}(\text{Sn}, \text{Fe})\text{O}_{3-\delta}$ showed small saturation magnetizations as compared with non-Ti substituted one, the magnetization increased a little with Ti doping rates up to 15%. On the other hand, all Ca-substituted $\text{Sr}(\text{Sn}, \text{Fe})\text{O}_{3-\delta}$ showed larger saturation magnetization than non-Ca substituted one. Two doublets of Fe^{3+} and a doublet of Fe^{4+} were observed in Mössbauer spectra of Ca-substituted $\text{Sr}(\text{Sn}, \text{Fe})\text{O}_{3-\delta}$ with weak ferromagnetism, and two sextets of high spin Fe^{3+} were additionally observed in Mössbauer spectra of Ca-doped $\text{Sr}(\text{Sn}, \text{Fe})\text{O}_{3-\delta}$ with relatively strong ferromagnetism. When $\text{Sr}(\text{Sn}, \text{Fe})\text{O}_{3-\delta}$ were further codoped with Ca and Ti ions, they showed the stable and enhanced ferromagnetic properties. It is considered that magnetic polarons among high spin Fe^{3+} species are overlapped by shrinking or deforming the crystal structure of perovskite oxides. That is the magnetism induced by a chemical pressure of perovskite oxides.

Keywords SrSnO_3 · Fe, Ca, Ti doping · Magnetic property · Unit cell volume · Mössbauer · Dilute magnetism · Chemical pressure · $\text{Sr}(\text{Sn}, \text{Fe}, \text{Ti})\text{O}_3$ · $(\text{Sr}, \text{Ca})(\text{Sn}, \text{Fe})\text{O}_3$ · $(\text{Sr}, \text{Ca})(\text{Sn}, \text{Fe}, \text{Ti})\text{O}_3$

This article is part of the Topical Collection on *Proceedings of the International Conference on the Applications of the Mössbauer Effect (ICAME 2017), Saint-Petersburg, Russia, 3–8 September 2017*
Edited by Valentin Semenov

✉ Kiyoshi Nomura
dqf10204@nifty.com

¹ Applied Chemistry, Meiji University, Higashi-Mita 1-1-1, Kawasaki, Kanagawa, 214-8571, Japan

² The University of Tokyo, Komaba, Meguro-ku, Tokyo, 153-8902, Japan

1 Introduction

Wide-bandgap oxide semiconductors and insulators such as ZnO, SnO₂, TiO₂, SiO₂, Al₂O₃ etc. doped with dilute magnetic ions have shown both magnetic and semiconductor behaviors at room temperature [1]. It is known that perovskite oxides with ABO₃ composition have interesting properties such as superconductivity, ferroelectricity, half metallicity, magnetism, and so on. Regarding to perovskite oxides, SrSn_{1-x}Fe_xO_{3-δ} ($x \leq 0.2$), the electrical conductivity and oxygen sensing behavior have already been reported [2]. The electrical conductivity increases with Fe doping rates as the activation energy decreases. According to a phase transition in perovskite SrSnO₃-SrFeO₃ solid solutions [3], the crystal structure depends on Fe contents. SrSn_{1-x}Fe_xO_{3-δ} doped with Fe ($x \leq 0.3$) have an orthorhombic structure, the samples doped with Fe ($x = 0.4-0.9$) have a cubic structure, and the end member of SrFeO_{2.74} has a tetragonal structure.

In contrast to the study on the conductive characteristics, there are only a few of papers concerning dilute magnetic properties of perovskite oxides. The magnetic and magneto-optical properties of Fe-doped BaTiO₃ films [4] and Fe-doped SrTiO₃ films [5] were reported. G. Prathiba et al. [6] studied on magnetic properties of SrSn_{1-x}Fe_xO_{3-δ} ($x = 0.03, 0.04, 0.05$) films, and showed that Curie temperatures of SrSn_{1-x}Fe_xO_{3-δ} with $x = 0.04$ and 0.05 are 618 and 638 K, respectively. The magnetic properties of SrSn_{0.9}Sb_{0.05}Fe_{0.05}O₃ film co-doped with Fe and Sb was also investigated [7]. Perovskite oxide, pure SrSnO₃, is a diamagnetic compound with the bandgap of 4.04 eV [8].

In order to confirm the dilute magnetism of SrSnO₃, we have studied the magnetic properties and crystal structures of SrSn_{1-x}Fe_xO_{3-δ} ($x = 0.01-0.15$) prepared systematically by a sol-gel and thermal decomposition method [9]. SrSn_{1-x}Fe_xO_{3-δ} with $x > 8\%$ showed ferromagnetism at room temperature and SrSn_{1-x}Fe_xO_{3-δ} with $x \leq 8\%$ showed very weak ferromagnetic behavior with major paramagnetic one. Mössbauer spectra of Fe-doped SrSnO₃ with the ⁵⁷Fe enrichment of 1% showed three doublets with tetra- and trivalent states for the small amounts of Fe doped ones, and additionally magnetic sextets for the large Fe doped ones.

In this report, the magnetic behavior of SrSn_{1-x}Fe_xO_{3-x} changed by substituting Sr in site A and Sn in site B of perovskite oxides (ABO₃) with non-magnetic Ca and Ti ions, respectively, were studied in order to clarify the dilute magnetism due to the crystal deformation or chemical pressure of perovskite oxides.

2 Experimental

Ti doped Sr(Sn_{0.9-y}Fe_{0.1}Ti_y)O_{3-δ} Ca doped (Sr,Ca)(Sn_{1-x}Fe_x)O_{3-δ} and Ti & Ca codoped (Sr, Ca)(Sn_{1-x-y}Fe_xTi_y)O_{3-δ} samples were prepared by a sol-gel method and annealed at 400 °C for 2 h and at 1000 °C for 2 h in air atmosphere [9]. Prepared samples were investigated by using a X-ray diffractometer (XRD: Rigaku Corporation), a vibration sample magnetometer (VSM: Riken Denshi Co.), and a ⁵⁷Fe Mössbauer spectrometer (Silas Inc.). Unit cell volumes were calculated from the lattice parameters obtained by XRD, assumed that SrSnO₃ crystals have an orthorhombic structure. The magnetic properties of saturation magnetization, residual magnetization and coercivity were estimated from the endpoints, longitudinal axis and horizontal axis intersections of VSM hysteresis loops, respectively. The velocity of Mössbauer spectra was calibrated by using a sextet of an α -Fe foil, and isomer shift (*IS*) values were relative to α -Fe. The linewidths of the three doublet components in the Mössbauer spectra were restricted to be equal.

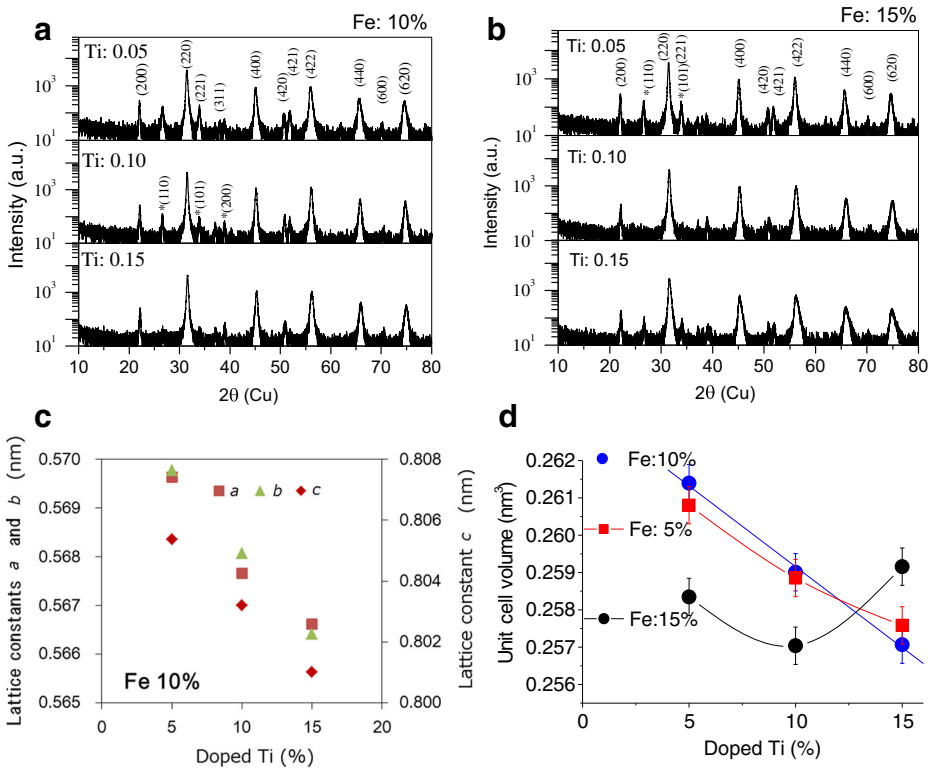


Fig. 1 XRD patterns of **a** $\text{Sr}(\text{Sn}_{0.90-y}\text{Fe}_{0.1}\text{Ti}_y)\text{O}_{3-\delta}$ and **b** $\text{Sr}(\text{Sn}_{0.85-y}\text{Fe}_{0.15}\text{Ti}_y)\text{O}_{3-\delta}$ doped with Ti ($y = 0.05, 0.1, \text{ and } 0.15$), **c** typical lattice constants of $\text{Sr}(\text{Sn}_{0.9-y}\text{Fe}_{0.1}\text{Ti}_y)\text{O}_{3-\delta}$ and **d** the unit cell volumes of $\text{Sr}(\text{Sn}_{1-x-y}\text{Fe}_x\text{Ti}_y)\text{O}_{3-\delta}$ ($x, y = 0.05, 0.1, 0.15$). *: trace peaks are assigned to SnO_2

3 Results and discussion

3.1 Ti doping effect of $\text{Sr}(\text{Sn,Fe})\text{O}_{3-\delta}$

$\text{Sr}(\text{Sn}_{1-x-y}\text{Fe}_x\text{Ti}_y)\text{O}_{3-\delta}$ doped with Fe ($x = 0.05, 0.1, \text{ and } 0.15$) and Ti ($y = 0.05, 0.1, \text{ and } 0.15$) were prepared. XRD patterns of $\text{Sr}(\text{Sn}_{0.9-y}\text{Fe}_{0.1}\text{Ti}_y)\text{O}_{3-\delta}$ and $\text{Sr}(\text{Sn}_{0.85-y}\text{Fe}_{0.15}\text{Ti}_y)\text{O}_{3-\delta}$ are shown in Fig. 1a and b, respectively. XRD patterns of almost all samples showed the orthorhombic structure of $\text{Sr}(\text{Sn}_{1-x-y}\text{Fe}_x\text{Ti}_y)\text{O}_{3-\delta}$ close to tetragonal structure except $\text{Sr}(\text{Sn}_{0.70}\text{Fe}_{0.15}\text{Ti}_{0.15})\text{O}_{3-\delta}$ although trace amounts of SnO_2 were sometimes included. Other impurity phases were not detected. Typical lattice parameters of $\text{Sr}(\text{Sn}_{0.90-y}\text{Fe}_{0.1}\text{Ti}_y)\text{O}_{3-\delta}$ ($y = 0.05, 0.1, \text{ and } 0.15$) are shown in Fig. 1c. When doped Fe contents were 5% and 10%, the lattice constants of $a, b, \text{ and } c$ decreased with Ti doping rates, and the unit-cell volumes decreased as shown in Fig. 1d. But for 15% Fe and 15% Ti codoped samples, the unit cell volume did not decrease monotonically because the orthorhombic structure was not close to the tetragonal for less 15% Ti codoping rates. As shown in Fig. 1b, the asymmetric peaks were observed especially in the high diffraction angle region.

The unit cell volumes of non-Ti doped samples were 0.261 nm^3 for 10% Fe doped sample and 0.260 nm^3 for 15% Fe doped one, respectively.

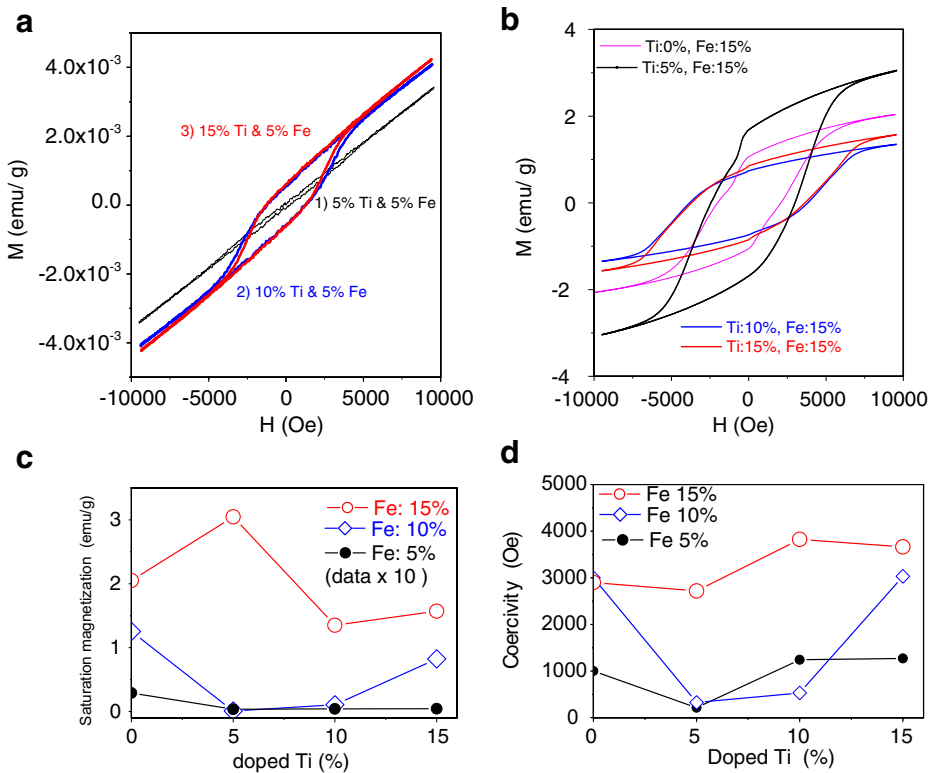


Fig. 2 VSM curves of **a** Sr(Sn_{0.95-y}Fe_{0.05}Ti_y)O_{3-δ} doped with (y = 0.05, 0.1, 0.15) and **b** Sr(Sn_{0.85-y}Fe_{0.15}Ti_y)O_{3-δ} doped with (y = 0.05, 0.1, 0.15) **c** saturation magnetization and **d** coercivity of Sr(Sn_{1-x-y}Fe_xTi_y)O_{3-δ}

Therefore, the cell volumes of almost all samples decrease with Ti doping rates. It is because the ionic radii of Fe³⁺ (0.0645 nm) and Ti⁴⁺ (0.061 nm) are smaller than Sn⁴⁺ (0.069 nm) and Fe and Ti ions are incorporated in perovskite oxides, SrSnO_{3-δ}. The highest Fe and Ti doped sample was much deformed orthorhombic phase ($a \neq b$), deviated from a tetragonal structure ($a \approx b$) because it may contain an orthorhombic phase with a little deviated composition or uncompleted substitution.

The magnetic properties of Ti doped Sr(Sn,Fe)O_{3-δ}, measured by VSM, are shown in Fig. 2. The magnetic properties for 5% Fe and 10% Fe doped samples with 5% to 15% Ti show weak ferromagnetic behavior with paramagnetic behavior, which have smaller saturation magnetization than non-Ti doped samples ($M_s = 0.029$ emu/g for 5% Fe doped SrSnO₃, $M_s = 1.25$ emu/g for 10% Fe doped SrSnO₃). Ti⁴⁺ is a non-magnetic ion, and does not interact with Fe³⁺ ions through oxygen atoms. However, with Ti doping rates, the saturation magnetization and coercivity increased a little. As for 15% Fe doped samples, the saturation magnetization increased by doping only 5% Ti ions (Fig. 2b). This is considered to be based on overlapping polarons between large amounts of Fe³⁺ with shrinking the unit cell by incorporating Ti ions with a small ionic radius [10]. However, a further doping of Ti up to 10% leads to the decrement of the saturation magnetization and the increment

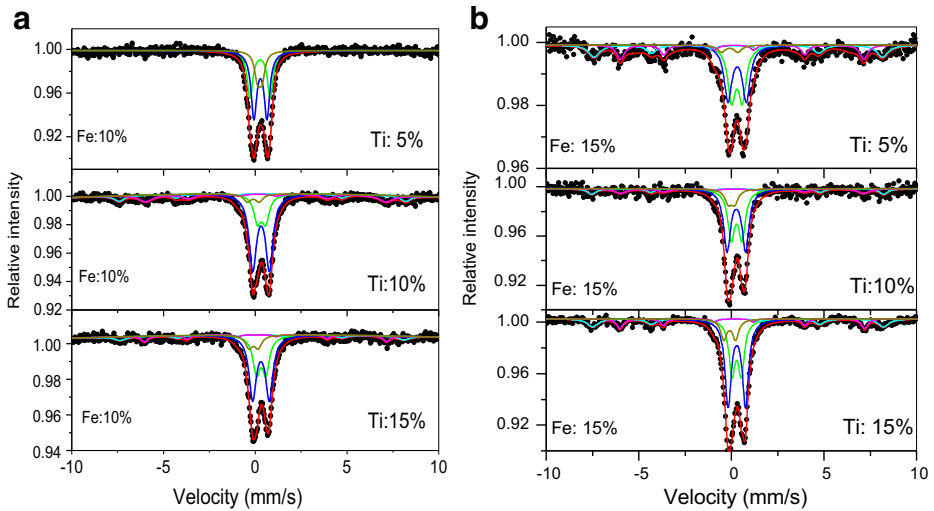


Fig. 3 Mössbauer spectra of **a** $\text{Sr}(\text{Sn}_{0.9-y}\text{Fe}_{0.1}\text{Ti}_y)\text{O}_{3-\delta}$ doped with Ti ($y = 0.05, 0.10, 0.15$) and **b** $\text{Sr}(\text{Sn}_{0.85-y}\text{Fe}_{0.15}\text{Ti}_y)\text{O}_{3-\delta}$ doped with ($y = 0.05, 0.10, 0.15$)

of the coercivity. The magnetic results for $\text{Sr}(\text{Sn}_{0.70}\text{Fe}_{0.15}\text{Ti}_{0.15})\text{O}_{3-\delta}$ are almost consistent with that of $\text{Sr}(\text{Sn}_{0.75}\text{Fe}_{0.15}\text{Ti}_{0.10})\text{O}_{3-\delta}$.

Mössbauer spectra of $\text{Sr}(\text{Sn}_{0.95-y}\text{Fe}_{0.05}\text{Ti}_y)\text{O}_{3-\delta}$ showed only paramagnetic peaks of Fe^{3+} and even for 10% Fe and 5% Ti doped sample the Mössbauer spectrum showed no magnetic sextet as shown in Fig. 3a. However, a weak ferromagnetic behavior with paramagnetic components was observed by means of VSM as shown in Fig. 2a. Almost all Fe species are assigned to paramagnetic Fe^{4+} and Fe^{3+} judging from the isomer shifts of doublets (D1 (Fe^{4+}) : $IS = -0.10$ mm/s, $QS = 0.61$ mm/s, Area Intensity (AI) = 12.6%, D2 (Fe^{3+}) : $IS = 0.28$ mm/s, $QS = 0.98$ mm/s, AI = 56.5%, D3 (Fe^{3+}) : $IS = 0.29$ mm/s, $QS = 0.46$ mm/s, AI = 30.8%), while Mössbauer spectrum of 10% Fe doped sample without Ti ions consisted of two or four sextets in addition to the paramagnetic doublets [9]. Even if this sample was measured at 6 K, no sextets appeared, and three doublets were observed. Of course, isomer shifts at 6 K increased by ca. 0.1 mm/s because of secondary order Doppler shift, and each QS value also increased due to deformation of an electric structure. If Fe^{3+} ions were incorporated into SrSnO_3 , oxygen vacancies should be produced at random in the structure of perovskite oxide according to the amount of Fe^{3+} contents.

When Ti ions were doped up to 10% and 15% for 10% Fe doped samples, magnetic sextets (M1: $IS = 0.30$ mm/s, $\varepsilon = 0.18$ mm/s, $B_{\text{hf}} = 48.5$ T, AI = 9.4%, M2: $IS = 0.30$ mm/s, $\varepsilon = 0.44$ mm/s, $B_{\text{hf}} = 40.7$ T, AI = 15.7%) appeared. This is interpreted due to overlapping polarons [11] enhanced by shorting the unit cell of perovskite oxides and by producing periodical oxygen vacancies. The pair sextets with hyperfine fields of 48 T and 41 T are considered due to Fe^{3+} occupying octahedral and tetrahedral sites, respectively. In Mössbauer spectra of 15% Fe doped samples as shown Fig. 3b, pair sextets with hyperfine fields of 48 T and 41 T were observed. The total area intensity of two sextets was 39% for 5% Ti doped sample, but 17.6% for 10% Ti doped sample and 22.1% for 15% Ti doped sample. The change of sextets' intensity is similar to that of magnetic behavior as shown in Fig. 2c although the real sextet intensity was smaller than non-Ti doped sample.

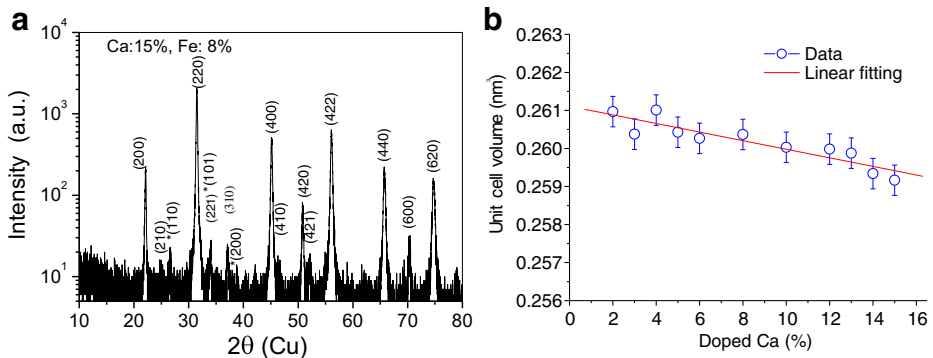


Fig. 4 Typical XRD pattern of 15% Ca doped $\text{Sr}(\text{Sn}_{0.92}\text{Fe}_{0.08})\text{O}_{3-\delta}$ and the unit cell volumes of $\text{Sr}(\text{Sn}_{0.92}\text{Fe}_{0.08})\text{O}_{3-\delta}$ doped with various concentrations of Ca

Only 5% Ti doping decreases so effectively the unit volume of perovskite oxide that the saturation magnetization for this sample exhibited larger value in comparison to non-Ti doped (2.05 emu/g) as shown in Fig. 2c.

3.2 Ca doping effect in $\text{Sr}(\text{Sn,Fe})\text{O}_{3-\delta}$

$\text{Sr}(\text{Sn}_{0.92}\text{Fe}_{0.08})\text{O}_{3-\delta}$ doped with Ca ions were prepared by the same sol-gel method and annealing at 1000 °C as that for $\text{Sr}(\text{Sn}_{0.92}\text{Fe}_{0.08})\text{O}_{3-\delta}$ samples. The typical XRD pattern of 15% Ca doped $\text{Sr}(\text{Sn}_{0.92}\text{Fe}_{0.08})\text{O}_{3-\delta}$ and the unit cell volumes of Ca doped $\text{Sr}(\text{Sn}_{0.92}\text{Fe}_{0.08})\text{O}_{3-\delta}$ are shown in Fig. 4. The unit cell volumes decreased clearly with Ca doping rates, of which the effect was somewhat weak as compared with Ti doping. The lattice parameters obtained from XRD data were much more deviated. The crystallite sizes were roughly estimated to be from 35 nm to 45 nm by Scherrer equation using the linewidth of XRD peaks.

The saturation magnetization and residual magnetization of $\text{Sr}(\text{Sn}_{0.92}\text{Fe}_{0.08})\text{O}_{3-\delta}$ doped with different Ca contents are shown in Fig. 5. As compared with non-Ca doped sample, all Ca doped $\text{Sr}(\text{Sn}_{0.92}\text{Fe}_{0.08})\text{O}_{3-\delta}$ show large saturation magnetizations. With Ca doping rates, the monotonic relationship between the saturation magnetization and Ca contents were not obtained.

Mössbauer spectra of $\text{Sr}(\text{Sn}_{0.92}\text{Fe}_{0.8})\text{O}_{3-\delta}$ doped with 12% Ca and without Ca are shown in Fig. 6. It shows that magnetic sextets were observed by doping with Ca ions. As for less than 8% Ca doping, the magnetic sextets were not clearly observed, but two sextets with hyperfine fields appeared by doping more than 10% Ca. Mössbauer spectra of more than 10% Ca doped samples exhibit three doublets and two sextets. Three doublets are composed of one Fe^{4+} ion and two Fe^{3+} ions. Two sextets with 48 T and 41 T are due to Fe^{3+} in octahedral and tetrahedral sites of perovskite oxides with oxygen defects, respectively.

3.3 Ca and Ti codoping effect of $\text{Sr}(\text{Sn,Fe})\text{O}_{3-\delta}$

Ca doping is actually effective in enhancing magnetic properties, though a simple relationship between magnetic properties and doping rates was not obtained. Ti doping

Fig. 5 Saturation magnetization and residual magnetization of $\text{Sr}(\text{Sn}_{0.92}\text{Fe}_{0.08})\text{O}_{3-\delta}$ doped with different Ca contents

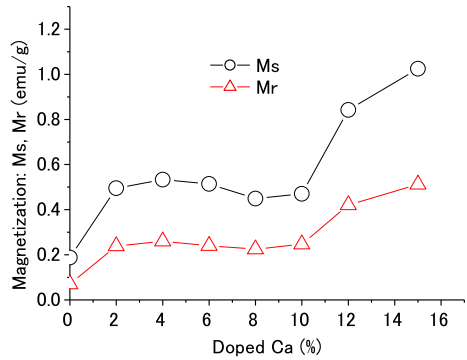


Fig. 6 Mössbauer spectra of $(\text{Sr}_{1-x}\text{Ca}_x)(\text{Sn}_{0.92}\text{Fe}_{0.08})\text{O}_{3-\delta}$ with $x = 0.0$ and 0.12

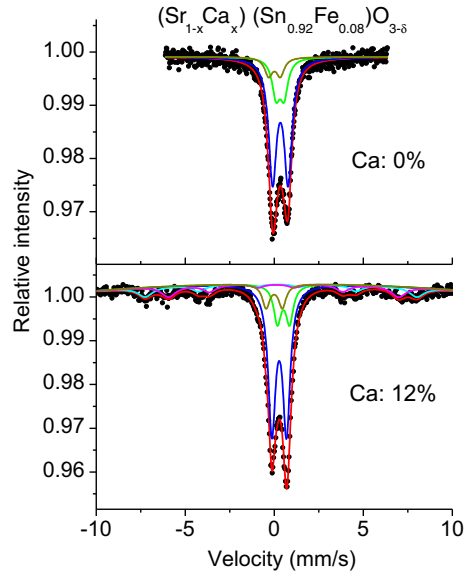


Fig. 7 Unit-cell volume of $(\text{Sr}_{0.88}\text{Ca}_{0.12})(\text{Sn}_{0.92-y}\text{Fe}_{0.08}\text{Ti}_y)\text{O}_{3-\delta}$ with $y = 0, 0.05, 0.10$ and 0.15 (Plotted data were average values for three measurements)

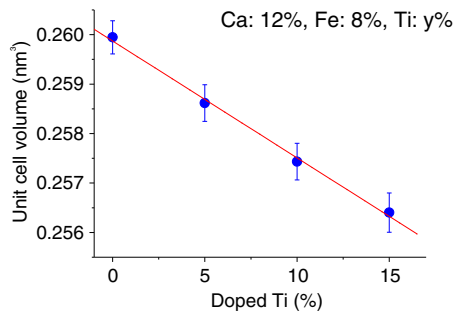


Fig. 8 Magnetization curves of $(\text{Sr}_{0.88}\text{Ca}_{0.12})(\text{Sn}_{0.92-y}\text{Fe}_{0.08}\text{Ti}_y)\text{O}_{3-\delta}$ with $y = 0.05, 0.10,$ and 0.15

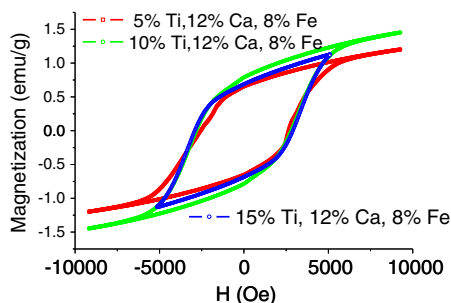
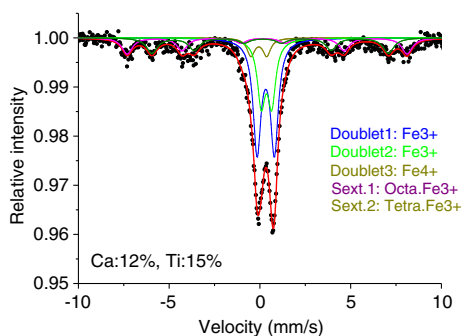


Fig. 9 Mössbauer spectrum of $(\text{Sr}_{0.88}\text{Ca}_{0.12})(\text{Sn}_{0.77}\text{Fe}_{0.08}\text{Ti}_{0.15})\text{O}_{3-\delta}$



is effective in shrinking the lattice constant of perovskite oxides, but not so effective in enhancing magnetic properties. Ca and Ti codoping effect was studied using $(\text{Sr}_{0.88}\text{Ca}_{0.12})(\text{Sn}_{0.92-y}\text{Fe}_{0.08}\text{Ti}_y)\text{O}_{3-\delta}$. The unit cell volumes estimated by XRD decreased linearly with Ti doping rates as shown in Fig. 7. The magnetic properties of $(\text{Sr}_{0.88}\text{Ca}_{0.12})(\text{Sn}_{0.92-y}\text{Fe}_{0.08}\text{Ti}_y)\text{O}_{3-\delta}$ with $y = 0.05, 0.10,$ and 0.15 are shown in Fig. 8. The VSM curves show magnetic hysteresis of ferromagnetic behavior in addition to paramagnetic behavior. The saturation magnetization and coercivity of these samples are almost the same in spite of different Ti doping rates. The unit cells shrank according to only Ti doping, which decreased the magnetic characteristics. It is considered that nonmagnetic Ti ions do not interact directly the high-spin electron orbit of Fe ions via oxygen atoms. However, Ca doping in the presence of Ti ions increased ferromagnetic properties although Fe contents were only 8%. It may be due to magnetic polarons.

Mössbauer spectrum of $(\text{Sr}_{0.88}\text{Ca}_{0.12})(\text{Sn}_{0.92-y}\text{Fe}_{0.08}\text{Ti}_y)\text{O}_{3-\delta}$ with $y = 0.15$ is shown in Fig. 9, which is a representative characteristics of the codoped samples. The doublets and sextets are assigned to the same Fe species as described in the previous section. Thus it is found that Ca and Ti codoping in $\text{Sr}(\text{Sn},\text{Fe})\text{O}_3$ gives the stable structure and enhanced magnetic properties.

Even if magnetic sextets were not observed in the Mössbauer spectra, authors have reported the similar results that SnO_2 samples doped with ^{57}Fe show the ferromagnetism [10].

4 Conclusions

Ca and Ti doped Sr(Sn,Fe)O_{3-δ} samples were prepared by a sol-gel method and the succeeding thermal annealing at 1000 °C, and showed the orthorhombic structure (close to tetragonal) of perovskite oxides with crystalline sizes of about 40 nm and ferromagnetism including paramagnetic components at room temperature. The unit cell volumes decreased with increasing Ti and Ca concentrations.

Ti doped Sr(Sn, Fe)O_{3-δ} showed small saturation magnetization, as compared with non-Ti doped one, but increased the magnetization a little with the increase of Ti doping rate. Ca doping in Sr(Sn, Fe)O_{3-δ} showed large saturation magnetization, as compared with non-Ca doped one, but the magnetic characteristics did not linearly increase with doping rates.

Ca substitution at site A of perovskite oxides enhanced effectively the magnetic properties for Sr(Sn, Fe)O₃. It is considered that the dilute magnetism enhanced is due to the structural shrinking or deformation induced by a chemical pressure of site A. It is found that Ca and Ti codoping provides a stable structure and enhances magnetic properties of perovskite oxides, Sr(Sn_{1-x}Fe_x)O_{3-δ}.

The chemical pressure effect for dilute magnetism was confirmed by substituting with Ca and Ti at A site and B site of perovskite oxides, respectively.

Acknowledgements Authors thank Dr. Norimichi Kojima in The Toyota Physical and Chemical Research Institute for supporting this study.

References

1. Nomura, K.: Magnetic properties and oxygen defects of dilute metal doped tin oxide based semiconductor. *Croat. Chem. Acta* **88**, 579–590 (2015)
2. Misra, S., Gnanasekar, K.I., Subba Rao, R.V., Jayaraman, V., Gnanasekaran, T.: Electrical conductivity and oxygen sensing behavior of SrSn_{1-x}Fe_xO_{3-δ} (x = 0–0.2). *J. Alloy. Comput.* **506**, 285 (2010)
3. Schmid Beurmann, P., Thangadurai, V., Weppner, W.: Phase transitions in the SrSnO_{3-δ}/SrFeO₃ solid solutions: X-ray diffraction and Mössbauer studies. *J. Solid State Chem.* **174**, 392–402 (2003)
4. Rajamani, A., Dionne, G.F., Bono, D., Ross, C.A.: Faraday rotation, ferromagnetism, and optical properties in Fe-doped BaTiO₃. *J. Appl. Phys.* **98**, 063907 (2005)
5. Kim, H., Bi, L., Dionne, G.F., Ross, C.A.: Magnetic and magneto-optical properties of Fe-doped SrTiO₃ films. *Appl. Phys. Lett.* **93**, 092506 (2008)
6. Prathiba, G., Venkatesh, S., Harish Kumar, N.: Structural, magnetic and semiconducting properties of Fe doped SrSnO₃. *Solid State Commun.* **150**, 1436 (2010)
7. Prathiba, G., Venkatesh, S., Kamala Bharathi, K., Harish Kumar, N.: Magnetic and transport properties of transparent SrSn_{0.9}Sb_{0.05}Fe_{0.05}O₃ semiconductor films. *J. Appl. Phys.* **109**, 07C320 (2011)
8. Bannikov, V.V., Shein, I.R., Kozhevnikov, U.L., Ivanovskii, A.L.: Magnetism without magnetic ions in non-magnetic perovskites SrTiO₃, SrZrO₃ and SrSnO₃. *J. Mag. Mag. Mater.* **320**, 936–942 (2008)
9. Nomura, K., Suzuki, S., Koike, Y., Hongling, L., Okazawa, A., Kojima, N.: Magnetic property and Mössbauer analysis of SrSn_{1-x}Fe_xO₃ prepared by a sol-gel method. *Hyperfine Interact.* **237**, 26 (2016)
10. Coey, J.M.D., Venkatesan, M., Fitzgerald, C.B.: Donor impurity band exchange in dilute ferromagnetic oxides. *Nat. Mater.* **4**, 173 (2005)
11. Nomura, K., Barrero, C., Sakuma, J., Takeda, T.: Room-temperature ferromagnetism of sol-gel-synthesized Sn_{1-x}⁵⁷Fe_xO_{2-δ} powders. *Phys. Rev. B* **75**, 184411 (2007)